



# Enhancing drug release from PEG-PLGA implants: The role of Hydrophilic Dexamethasone Phosphate in modulating release kinetics and degradation behavior

Eric Lehner<sup>a,f</sup>, Marie-Luise Trutschel<sup>b</sup>, Matthias Menzel<sup>c</sup>, Jonas Jacobs<sup>d</sup>, Julian Kunert<sup>b</sup>, Jonas Scheffler<sup>a</sup>, Wolfgang H. Binder<sup>e</sup>, Christian E.H. Schmelzer<sup>b,c</sup>, Stefan K. Plontke<sup>a,f</sup>, Arne Liebau<sup>a,1</sup>, Karsten Mäder<sup>b,f,\*</sup>

<sup>a</sup> Department of Otorhinolaryngology-Head and Neck Surgery, Martin Luther University Halle-Wittenberg, Ernst-Grube-Straße 40 06120 Halle (Saale), Germany

<sup>b</sup> Institute of Pharmacy, Martin Luther University Halle-Wittenberg, Wolfgang-Langenbeck-Straße 4 06120 Halle (Saale), Germany

<sup>c</sup> Fraunhofer Institute for Microstructure of Materials and Systems IMWS, Walter-Hülse-Straße 1 06120 Halle (Saale), Germany

<sup>d</sup> Institute of Chemistry, Martin Luther University Halle-Wittenberg, Kurt-Mothes-Straße 2 06120 Halle (Saale), Germany

<sup>e</sup> Institute of Chemistry, Martin Luther University Halle-Wittenberg, Von-Danckelmann-Platz 4 06120 Halle (Saale), Germany

<sup>f</sup> Halle Research Centre for Drug Therapy (HRCdT), Halle (Saale), Germany

## ARTICLE INFO

### Keywords:

Dexamethasone  
PLGA  
Hot-melt extrusion  
Controlled release  
Implant  
Polymer degradation

## ABSTRACT

Poly(lactic-co-glycolic acid) (PLGA) is a prominent biodegradable polymer used in biomedical applications, including drug delivery systems (DDS) and tissue engineering. PLGA's ability to control drug release is often hindered by nonlinear release profiles and slow initial drug release for hydrophobic drugs. This study investigates the incorporation of dexamethasone phosphate (DEXP) into polyethylene glycol-poly(lactic-co-glycolic acid) (PEG-PLGA) implants to enhance the initial release rate of dexamethasone (DEX). Implants were fabricated via hot-melt extrusion with varying DEX to DEXP ratios. X-ray diffraction (XRD) analysis confirmed that DEX remained crystalline in all formulations, whereas DEXP's crystallinity was detectable only in higher concentrations. Energy-dispersive X-ray spectroscopy (EDX) provided insights into the distribution of DEX and DEXP within the polymer matrix. Drug release studies revealed that PEG-PLGA implants accelerated initial drug release with increasing quantity of DEXP, though it also led to a shorter overall release duration. Despite these improvements, all implants exhibited a biphasic release profile. DEXP also influenced the characteristics of the polymer matrix, evidenced by increased swelling, water absorption, and mass loss. <sup>1</sup>H NMR analysis revealed a faster decrease in glycolic acid monomers in DEXP-containing implants. These findings demonstrate that DEXP enhances early drug release of DEX-loaded PEG-PLGA implants prepared by hot-melt extrusion. However, balancing initial and sustained release profiles remains challenging.

## 1. Introduction

Poly(lactic-co-glycolic acid) (PLGA) is a biodegradable and biocompatible polymer that has garnered significant attention in the biomedical field, particularly for its applications in drug delivery systems (DDS) and tissue engineering (Anderson and Shive, 1997; Gentile et al., 2014; Klose et al., 2008). Its unique properties, including tunable degradation rate, mechanical strength, and ability to encapsulate a wide range of therapeutic agents led to its dominating role in the field of

biodegradable, implantable devices (Kapoor et al., 2015; Park, 1994). The ability to modulate the drug release rate and degradation time of PLGA implants from days to months is achieved through modifications in the size and geometry of the DDS, as well as the polymer's chemical composition, including the monomer ratio and molecular weight (Bassand et al., 2022; Bode et al., 2019). However, PLGA-based systems often face challenges like undesired nonlinear drug delivery profiles. For hydrophobic drug molecules initial lag times during the first days or weeks are observed (Janich et al., 2019; Wischke and Schwendeman,

\* Corresponding author at: Institute of Pharmacy, Martin Luther University Halle-Wittenberg, Wolfgang-Langenbeck-Straße 4 06120 Halle (Saale).

E-mail address: [karsten.maeder@pharmazie.uni-halle.de](mailto:karsten.maeder@pharmazie.uni-halle.de) (K. Mäder).

<sup>1</sup> These authors contribute equally.

2008; Zlomke et al., 2019). The incorporation of plasticizers like ethyl pyruvate and polypropylene glycol (PEG) avoids such undesirable lag phases (Lehner et al., 2019; Šnejdrová et al., 2021; Steele et al., 2011). However, these plasticizers often induce plastic deformation, permanently compromising the implant's structural integrity under stress and thus compromising their structural integrity during handling (Lehner et al., 2023; Steele et al., 2011). In contrast, polyethylene glycol-poly(lactic-co-glycolic acid) (PEG-PLGA) implants demonstrated elastic behavior, allowing them to recover their original shape after mechanical stress (Lehner et al., 2023). Furthermore, PEG-PLGA polymers prevented acidic microenvironment formation and provided more consistent drug release compared to their PLGA counterparts (de Souza et al., 2021; Lehner et al., 2024; Milacic and Schwendeman, 2014; Witt et al., 2000). However, the initial slow release of dexamethasone (DEX)-loaded PEG-PLGA hot-melt extrudates was still observed even after an additional plasticizer was incorporated (Lehner et al., 2023). An alternative strategy to address the slow initial drug release included the incorporation of high water-soluble salts (Patel et al., 2012; Webber et al., 1998; Zhang et al., 1997). PLGA microparticles loaded with more hydrophilic dexamethasone sodium phosphate (DEXP) showed a significantly faster release in the first 10 days compared to the DEX counterparts (Zhang and Bodmeier, 2023). Qnouch et al. (2021) demonstrated that adding DEXP to DEX-loaded silicone-based systems increased initial release rates. Since only dissolved drug molecules can diffuse out of the DDS, using the more hydrophilic DEXP was expected to enhance water penetration, improve drug dissolution, and facilitate its diffusion. While this approach showed promising results in silicone-based implants, its applicability to biodegradable polymers involves additional complexities, such as swelling, degradation, and erosion kinetics (Fredenberg et al., 2011). The use of DEXP may have further benefits for intracochlear drug delivery where DEX is released in the basal part of the scala tympani in the cochlea. The high permeability of DEX allows for quick uptake into the target cells of the inner ear, but this also leads to rapid elimination from the perilymphatic fluid space of scala tympani (half-life 46 min) (Salt et al., 2018). In contrast, DEXP, due to its hydrophilic nature, exhibits slower initial cellular uptake, allowing for better distribution along the scala tympani towards apical regions. However, DEXP is a prodrug and remains inactive until phosphatases cleave its polar phosphate group, converting it to the active form, DEX. Other potential applications seem feasible as well, such as intravitreal administration in the eye. The FDA-approved Ozurdex® implant, containing 0.7 mg of DEX in a PLGA matrix, has been used for treating macular edema and non-infectious uveitis. However, its current design still offers room for improvement in release kinetics (Bhagat et al., 2014; Costello et al., 2023; Lehner et al., 2019), highlighting the potential benefits of exploring modified formulations such as those investigated in this study.

This study aims to explore the design, fabrication, and characterization of PEG-PLGA implants with varying ratios of DEX and DEXP, focusing on fast initial drug release. This study utilized a range of analysis techniques, including optical microscopy, X-ray diffraction, gravimetric analysis, gel permeation chromatography, proton nuclear magnetic resonance spectroscopy, energy-dispersive X-ray spectroscopy, and *in vitro* drug release measurements, to comprehensively characterize these implants and evaluate their performance.

## 2. Material and methods

### 2.1. Materials

Expansorb® 10P037 DLG50-6P (polyethylene glycol-poly(lactic-co-glycolic acid); PEG-PLGA; lactic acid:glycolic acid (50:50); inherent viscosity 0.55–0.70 dL/g; molecular weight range 36–77 kDa; molecular weight of PEG 5 kDa) was purchased from Seqens (Ecully Cedex, France). Micronized dexamethasone (DEX) and dexamethasone phosphate disodium salt (DEXP) were bought from Caesar & Loretz GmbH

(Hilden, Germany). Dulbecco's Phosphate Buffered Saline (PBS) was used as an incubation medium. All other chemicals and solvents were of analytical or chromatographic grade and used without further purification.

### 2.2. Implant preparation using hot-melt extrusion

PEG-PLGA was milled for four cycles of 90 s each in a cryo-mill (Retsch GmbH, Haan, Germany) with a frequency of 25 Hz. The pulverized polymer and selected ratios of micronized drugs underwent a second milling for 90 seconds at 15 Hz. Hot-melt extrusion was performed using a ZE 5 ECO extruder equipped with a 0.3 mm die (Three-Tec GmbH; Seon; Switzerland) with a screw frequency of 80 rpm. The process temperatures of the three heating zones were maintained constant at 58, 58, and 62 °C (from feeding zone to die). The extrudates were collected and manually cut into pieces measuring 3 mm (equivalent to 0.4 mg) or 7.5 mm (equivalent to 1 mg), then stored at –20 °C. Microscopic images of the implants were captured using a Zeiss Axio Zoom.V16 microscope. Dimensions were determined in triplicate using Zen 3.1 software (Carl Zeiss, Oberkochen, Germany).

### 2.3. Electron beam irradiation

Electron beam irradiation was selected as the sterilization process. Implants were irradiated using a 10 MeV linear accelerator MB 10–30 MP (Mevex, Ontario, Canada) on a moving tray (95 cm/min) at room temperature. The accelerator operated at a repetition rate of 460 Hz, generating 8 μs pulses, and utilized a scanning frequency of 3 Hz with a scanning width of up to 60 cm. A total dose of 25 kGy was administered by applying two separate doses of 12.5 kGy each.

### 2.4. X-ray diffraction (XRD)

X-ray diffraction experiments were performed to investigate the crystallinity of DEX and DEXP in the extrudates. For this, a D2-Phaser powder diffractometer operating in Bragg-Brentano geometry with a LYNXEYE XE-T Strip Detector was used. The device was equipped with a copper anode (30 kV and 10 mA) and Cu Kα<sub>1,2</sub> radiation (0.15406 nm, 0.15444 nm) was used. Data of the rotating samples were collected at a range of 2θ = 8–35° with an angular resolution of 0.02° and a total acquisition time of 1 h. The diffraction patterns were processed using the Bruker DIFFRAC.EVA software package (V7.1). All samples were prepared on low background sample holders made from specially oriented single crystalline silicone. For sample adhesion, a thin layer of Baysilone® silicone grease was applied to the surface of the sample holder. Samples were then directly spread on the silicone grease layer.

### 2.5. Drug distribution within implant cross-sections

Scanning electron microscopy (SEM) coupled with energy-dispersive X-ray spectroscopy (EDX) was employed to assess the morphology and drug distribution within implant cross-sections. The analysis was conducted using a Quanta 3D FEG scanning electron microscope (FEI Company, Eindhoven, Netherlands) equipped with an Oxford Xplore EDX-Detector (Oxford Instruments, Abingdon, UK). Implants were cryofractured using liquid nitrogen to preserve structural integrity and prevent artifacts caused by deformation. The samples were then mounted onto adhesive carbon conduction tabs (PlanoCarbon; Plano GmbH, Wetzlar, Germany) and sputter-coated with palladium to enhance surface conductivity for imaging. Imaging of the cross-sections was performed at accelerating voltages ranging from 2 to 5 keV and beam currents between 22 and 57 pA, utilizing the secondary electron signal. For EDX analysis, higher accelerating voltages of 10 keV and currents up to 3 nA were applied. EDX mappings were generated using AZtec V6.1 control software (Oxford Instruments, Abingdon, UK) and were visualized as false color images. Noise reduction was subsequently

carried out using Adobe Photoshop (Creative Cloud version; Adobe Inc., San José, CA, USA).

## 2.6. High performance liquid chromatography (HPLC)

A modified method from [AlAani and Alnukkary \(2016\)](#) was used for the simultaneous identification and quantification of DEX and DEXP. Drug concentrations were measured by HPLC analysis using a Jasco system (PU-1580 Pump; AS-1559 Intelligent Auto Sampler; UV-1559 Intelligent UV/VIS Detector; all Jasco, Oklahoma City, USA). The separation of DEX and DEXP was achieved using a LiChrospher® 100 RP-8 (5 µm) LiChroCART® 250-4 column (Merck KGaA, Darmstadt, Germany) operated at 40 °C. The isocratic mobile phase consisted of a mixture of acetonitrile and potassium dihydrogen phosphate buffer (0.05 M; 35:65) with a flow rate of 1 mL/min. 20 µL of the sample were injected and analyzed at  $\lambda = 239$  nm. Data recording and processing were carried out with the software ChromNAV Ver.2 (Jasco).

## 2.7. Drug load

Samples from different parts of the extruded material were collected and dissolved under vortexing in 100 µL of acetone and filled up to 1 mL with acetonitrile. The solutions were analyzed by HPLC to determine the drug load. Mean values and standard deviations were calculated from three replicate determinations and are reported.

## 2.8. Drug release

1 mg of each implant formulation was placed in 1.5 mL glass vials filled with 1 mL PBS and gently agitated in a water bath shaker under light-protected conditions (Precision SWB 15, Thermo Fisher Scientific, Waltham, MA, USA) at 37 °C. The total sample solution was withdrawn daily and analyzed using HPLC. An appropriate volume of PBS was replaced after taking samples. Experiments were conducted in triplicate.

## 2.9. Investigation of swelling

Implants were incubated in 1 mL PBS in 24-well cell culture plates. Samples were maintained at 37 °C in a shaker incubator at 25 rpm (Heidolph Promax 1020 coupled with Heidolph Incubator 1000, Schwabach, Germany). Microscopic images of the implants in wet conditions were captured for 28 days using a Zeiss Axio Zoom.V16 microscope. Changes in the implant diameter were determined using Zen 3.1 software (Carl Zeiss, Oberkochen, Germany). PBS was refreshed daily. Experiments were conducted in triplicate.

## 2.10. Implant erosion/degradation and water uptake

Implants were incubated as described in 2.9. After 3, 7, 10, 14, 21, and 28 days, implants were withdrawn carefully, blotted with tissue, weighed ( $m_{wet}$ ) and dried in a desiccator by applying vacuum for 48 h. Dried implants were analyzed for remaining mass ( $m_{dry}$ ) by gravimetric analysis. Polymer degradation was assessed using gel permeation chromatography (GPC) and proton nuclear magnetic resonance ( $^1H$  NMR) spectroscopy. Water uptake was calculated by [Eq. \(1\)](#):

$$\text{Water uptake [\%]} = \frac{m_{wet} - m_{dry}}{m_{dry}} * 100\% \quad (1)$$

PBS was refreshed daily until examination. All experiments were performed in triplicate, except for  $^1H$  NMR measurements, where three individual samples were combined to form a single pooled sample for analysis.

## 2.11. Gel permeation chromatography (GPC)

The molecular weight of PEG-PLGA was determined by a Viscotek

GPCmax VE 2001 system (Malvern Panalytical GmbH, Kassel, Germany) applying a CLM3008 precolumn, a CLM3008 main column, and a VE 3580 RI refractive index detector. Tetrahydrofuran (THF) was used as a carrier solvent with a sample concentration of 3 mg/mL. The flow rate was set to 1 mL/min. Polystyrene standards (PS) with a molecular weight range from 0.3 to 170 kg/mol (polydispersities <1.05) were used for calibration. Samples were filtered (PTFE-filters; 0.22 µm) before measuring.

## 2.12. Proton nuclear magnetic resonance ( $^1H$ NMR) spectroscopy

The  $^1H$  NMR measurements were performed at 400 MHz with VNMRS (Agilent Technologies, Santa Clara, USA). Deuterated chloroform ( $CDCl_3$ ) was used as carrier solvent with a sample concentration of 2–5 mg/mL. Mnova 14.2 (Mestrelab Research, Santiago de Compostela, Spain) was used to process the spectra and Origin 9.0 (OriginLab, Northampton, USA) was used for data integration. For spectral integration, the peaks corresponding to DEX were first identified. Then, the signals from PEG-PLGA or degradation products of PEG-PLGA were piecewise integrated. Only areas without DEX signals were used. Finally, the amount of PEG, lactic and glycolic parts were calculated from the integrals. For the assignment of the PEG-PLGA and its degradation products, an open-source NMR prediction tool was used ([Binev et al., 2007](#); "<https://www.nmrdb.org/>”).

## 3. Results and discussion

### 3.1. Characterization of drug loaded implants

This study aimed to characterize the influence of hydrophilic DEXP on the drug release profiles in DEX loaded PEG-PLGA implants. Therefore, various extrudates with increasing concentrations of DEXP were prepared using hot-melt extrusion ([Table 1](#)). The total drug content consistently remained at 10 % (w/w). [Fig. 1](#) illustrates all extrudate types examined in this study. All extrudates exhibited a golden-brown color resulting from the combination of the brown raw polymer and the integrated white drug powder. The manufacturing process was reproducible, resulting in only minimal differences in the diameter of the respective formulations ([Table 1](#)). The smallest diameter was found to be  $344 \pm 3.3$  µm for DEX8.75, and the largest was  $367 \pm 5.5$  µm for DEX5. Since diameter influences release kinetics, ensuring no significant variation between formulations is crucial ([Bassand et al., 2022](#)). Consequently, all samples were produced under similar conditions, including room temperature, humidity, extrusion temperature, and screw frequency. The diameter of the extrudates was larger than the die size (300 µm), which is a common characteristic of viscoelastic polymers. ([Wang, 2012](#); [Witt et al., 2000](#)). Nevertheless, all samples showed a uniform enlargement of the diameter. After cutting into 3 mm and 7.5 mm pieces, the implants were irradiated with an electron beam.

XRD was used to investigate the physical state of the drugs embedded in the implants. The milling process and extrusion temperature in the manufacturing process are expected to influence the crystallinity of both drugs. During milling, mechanical forces could induce changes in the crystal structure, potentially leading to partial or complete amorphization ([Oliveira et al., 2018](#)). [Zhang and Bodmeier \(2023\)](#) described that

**Table 1**

Composition of prepared implants and their respective diameters. Numbers in the formulation name represent the amount of DEX.

Formulation	PEG-PLGA [%]	DEX [%]	DEXP [%]	Diameter [µm]
DEX10	90	10	0	$354 \pm 1.6$
DEX8.75	90	8.75	1.25	$344 \pm 3.3$
DEX7.5	90	7.5	2.5	$348 \pm 9.4$
DEX6.25	90	6.25	3.75	$349 \pm 4.8$
DEX5	90	5	5	$367 \pm 5.5$

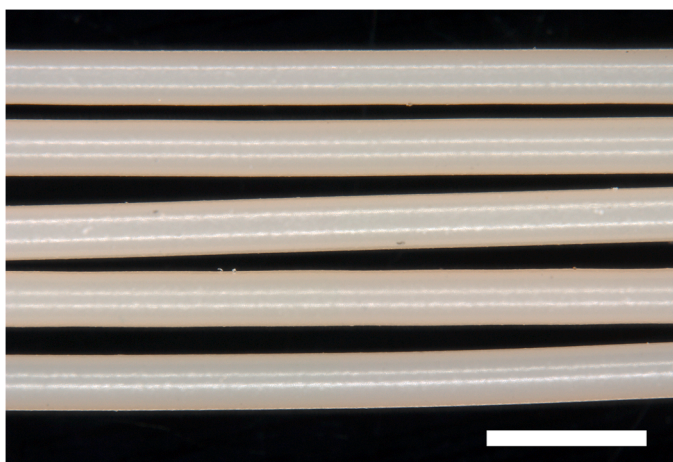


**Fig. 1.** Representative microscopic images illustrating the morphology of hot-melt PEG-PLGA extrudates with varying DEX and DEXP concentrations. From top to bottom: DEX10, DEX8.75, DEX7.5, DEX6.25, and DEX5. Scale bar represents 1 mm.

milled nanosized DEX showed characteristic peaks of a mixture of its polymorph forms A and B. Similarly, elevated temperatures during processing could cause changes in a crystalline state, either by facilitating recrystallization, transitions between crystalline polymorphs, or by inducing amorphous transitions. These alterations in crystallinity could significantly affect the stability and release rates of the drugs. X-ray powder diffraction patterns of both drugs, physical mixtures (PM), and implants are displayed in Fig. 2. Characteristic diffraction patterns of DEX were found in all implants with a drug load of 5 % to 10 %, identifying the drug in the crystalline state.

Moreover, no signs of polymorphic transformation were observed within the resolution of the device used, indicating that the crystalline structure of DEX remained unaffected by both milling and extrusion temperatures. In contrast, crystalline DEXP could only be detected in the DEX5 formulation containing 5 % DEXP. The signal of DEXP at 15.5° is clearly detectable; however, other characteristic peaks, including the prominent one at 13.4°, are not distinctly observed. This absence complicates the unambiguous identification of crystalline DEXP within the samples and is likely due to overlap with the DEX peak caused by strong

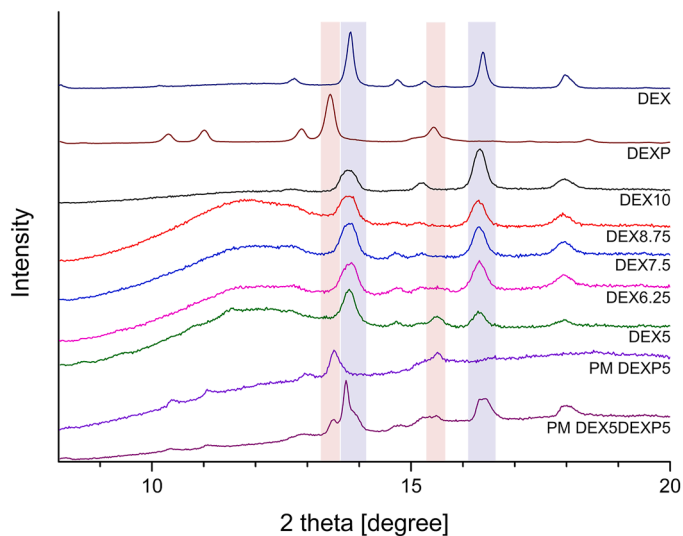


**Fig. 2.** X-ray diffraction patterns of dexamethasone (DEX), dexamethasone phosphate (DEXP), drug-loaded implants, and selected physical mixtures (PM). The blue and brown bars correspond to the most distinctive reflections of DEX and DEXP, respectively.

reflection broadening. This broadening is attributed to height displacement errors, as the XRD scans were conducted on implants with a diameter of 350  $\mu\text{m}$ . The sample geometry and the resulting height displacement error were intentionally applied to investigate the formulation itself without additional mechanical or temperature manipulation (e.g., (cryo)milling), which could otherwise affect the crystallinity of both DEX and DEXP (MacFhionnghaile et al., 2014). This lack of detection of DEXP is consistent with the results observed in PLGA microparticles (Zhang and Bodmeier, 2023). The evidence regarding the crystallinity of DEXP in implants with lower DEXP concentrations than 5 % is limited. The presence of crystalline DEXP in the DEX5 formulation could potentially result in increased mechanical stiffness and slower release rates, as crystalline structures dissolve more slowly compared to amorphous regions (Murdande et al., 2010). However, the DEX5 implants showed no noticeable differences in handling properties, and the water solubility of DEXP is likely sufficient to ensure that the crystalline regions dissolve quickly enough. Furthermore, the retention of DEX's crystalline state is expected to contribute to a slower but more predictable and controlled drug release profile.

The broad increase in background intensity with a maximum at 11.75° is attributed to the silicone grease used for sample adhesion (data not shown).

EDX was employed to visualize the distribution of both drugs within the polymer matrix. By detecting X-rays emitted from the sample upon electron beam bombardment, the technique enables the identification and mapping of specific elements. Both DEX and DEXP contain fluorine, while DEXP additionally possesses covalently bound phosphorus and ionically bound sodium, enabling its differentiation from DEX. The polymer PEG-PLGA comprises exclusively carbon, oxygen, and hydrogen. Fig. 3A presents a homogenous morphology of the DEX5 implant cross-section, with the red square indicating the EDX analysis region. The results of the EDX analysis of the selected area are shown in Fig. 3B. The spectrum displays the K ratio for each element, which represents the ratio of characteristic X-ray intensities emitted by the sample. The accompanying table provides the atomic ratios, explaining the differences between peak areas in the spectrum and the calculated atomic percentages. Despite the presence of fluorine in both drugs, its detection was relatively weak due to its low atomic number and consequent low X-ray emission (Moseley's law). In contrast, the key elements sodium and phosphorus in DEXP were detected more distinctly. The 2:1 sodium-to-phosphorus atomic ratio indicated the presence of DEXP (C<sub>22</sub>H<sub>28</sub>FN<sub>2</sub>O<sub>8</sub>P). However, the fluorine-to-phosphorus ratio deviated from the expected 2:1 ratio, as the implants were formulated based on mass rather than molar drug ratios.

Elemental mapping of the covalently bound atoms fluorine (F), phosphorus (P), and their combination (F + P) is depicted in Fig. 3C. Orange and purple dots represent fluorine and phosphorus, respectively. Overlaid maps of fluorine and phosphorus (F + P) highlighted DEXP-rich areas (purple and orange) while solely orange regions indicate DEX. Particles had a diameter smaller than 10  $\mu\text{m}$  and were uniformly dispersed within the PEG-PLGA matrix. Previous studies have also reported homogeneous DEX distribution in PLGA-based implants (Bendicho-Lavilla et al., 2023; Lehner et al., 2019; Saraf et al., 2023). Unfortunately, drug localization was feasible only in DEX5 implants, as sodium and phosphorus detection diminished with decreasing DEXP content. The intensity of fluorine remained consistently poor. A significant limitation of the measurement was the polymer's substantial alteration induced by the high-energy input.

The poor resolution of DEXP in XRD measurement may result from the conversion of DEXP to DEX during manufacturing or sterilization. While EDX analysis detected fluorine, sodium, and phosphorus in the true ratios, conversion processes cannot be ruled out. Therefore, the drug load for each formulation was determined at random sections of the extrudate strands. A modified method from AlAani and Alnukkary (2016) was used for the simultaneous identification and quantification of DEX and DEXP. Retention times for DEXP and DEX were 3.6 min and

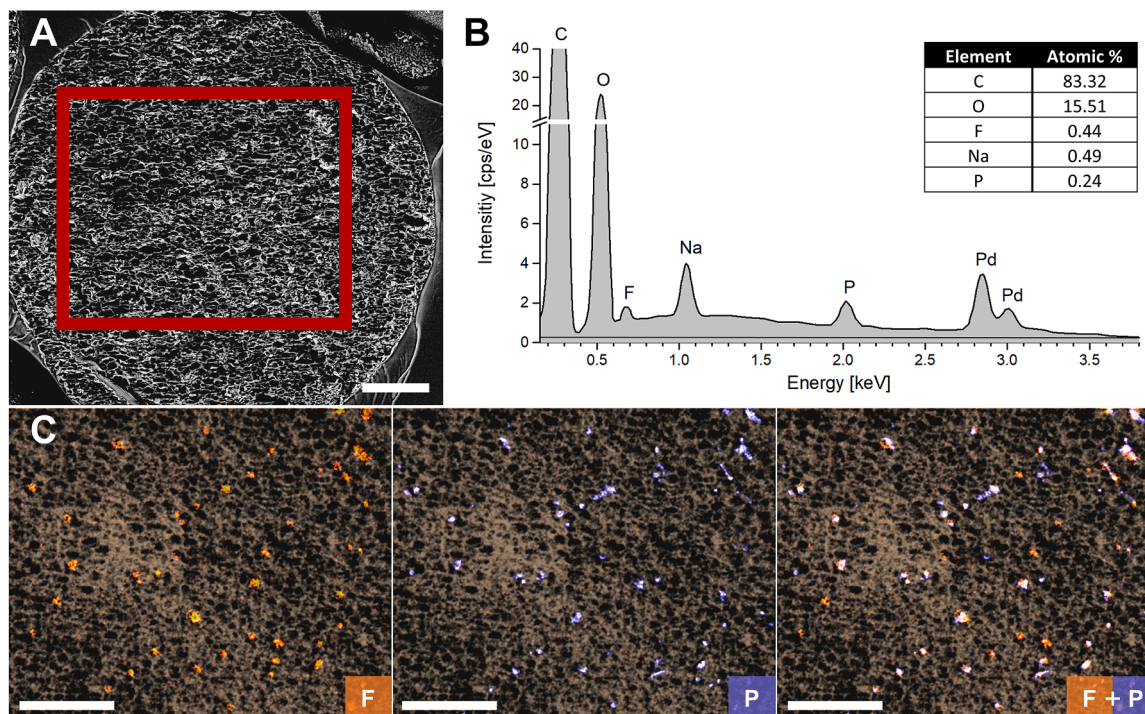


**Fig. 3.** SEM image of a DEX5 implant cross section (A) with the corresponding EDX spectrum (B) and elemental mapping analysis (C). The red square indicates the area of the EDX analysis. The orange dots represent the distribution of fluorine atoms, while the purple dots represent the distribution of phosphorus atoms. Scale bars indicate 50  $\mu\text{m}$ .

7.6 min, respectively. The drug loads of the respective formulations are shown in Fig. 4. The defined amounts of the drugs were recovered, ruling out the transformation of DEX to DEXP or drug inactivation. The low standard deviations indicate a homogeneous distribution of DEX and DEXP in the extruded material.

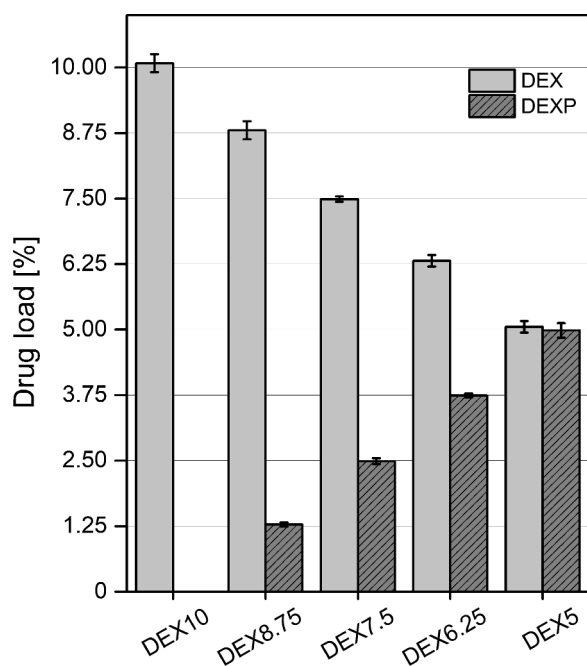


**Fig. 4.** Drug loading (% m/m) of DEX and DEXP in PEG-PLGA implants (mean  $\pm$  SD,  $n = 3$ ).

### 3.2. *In vitro* drug release

This study aimed to enhance the initial drug release of PEG-PLGA implants by incorporating water-soluble DEXP based on the hypothesis that increasing the hydrophilicity of the DDS would facilitate water uptake, thereby accelerating drug dissolution and diffusion. Immediate drug release from implants is essential for applications such as the management of acute ocular inflammation (uveitis) and the mitigation of foreign body responses to cochlear implant electrode arrays (Bode et al., 2018; Lehner et al., 2022). Therefore, the characterization of the release kinetics was focused on the initial days of drug release. Fig. 5A illustrates the release of DEX and DEXP from PEG-PLGA implants over 30 days, with more detailed visualization for the first 10 days (Fig. 5B). Drug release kinetics were consistently biphasic across all formulations, regardless of the DEX to DEXP ratio. An initial phase of approximately 10 days exhibited a constant release rate, followed by a period of accelerated drug release. Surprisingly, an initial burst release was not detected. In contrast, Zhang and Bodmeier (2023) demonstrated that 40 % of DEXP was released from 20 to 50  $\mu\text{m}$  PLGA microparticles within 5 days. However, the release profile of implants and microparticles is influenced by factors such as size, shape, porosity, and surface area. The manufacturing method significantly affects the implant's properties. Hot-melt extrusion creates smooth, non-porous surfaces, leading to slower drug release. Injection molding, on the other hand, produces surfaces with visible drug particles, resulting in faster drug release (McConville et al., 2015). Qnouch et al. (2021) reported a significant increase in release rate by adding DEXP to DEX-loaded silicone films and injection-molded implants, but the effect was less pronounced compared to microparticles. The prepared hot-melt PEG-PLGA implants demonstrated a similar trend (Fig. 5B). Implants with the highest DEXP concentration exhibited a cumulative drug release of 9.9 % after 10 days, compared to only 2.5 % for pure DEX implants. Daily release profiles revealed a consistent pattern across all formulations (Fig. 5C & D). An initial release on day 1 was more prominent for formulations with higher DEXP content, likely due to the presence of pure drug particles at the

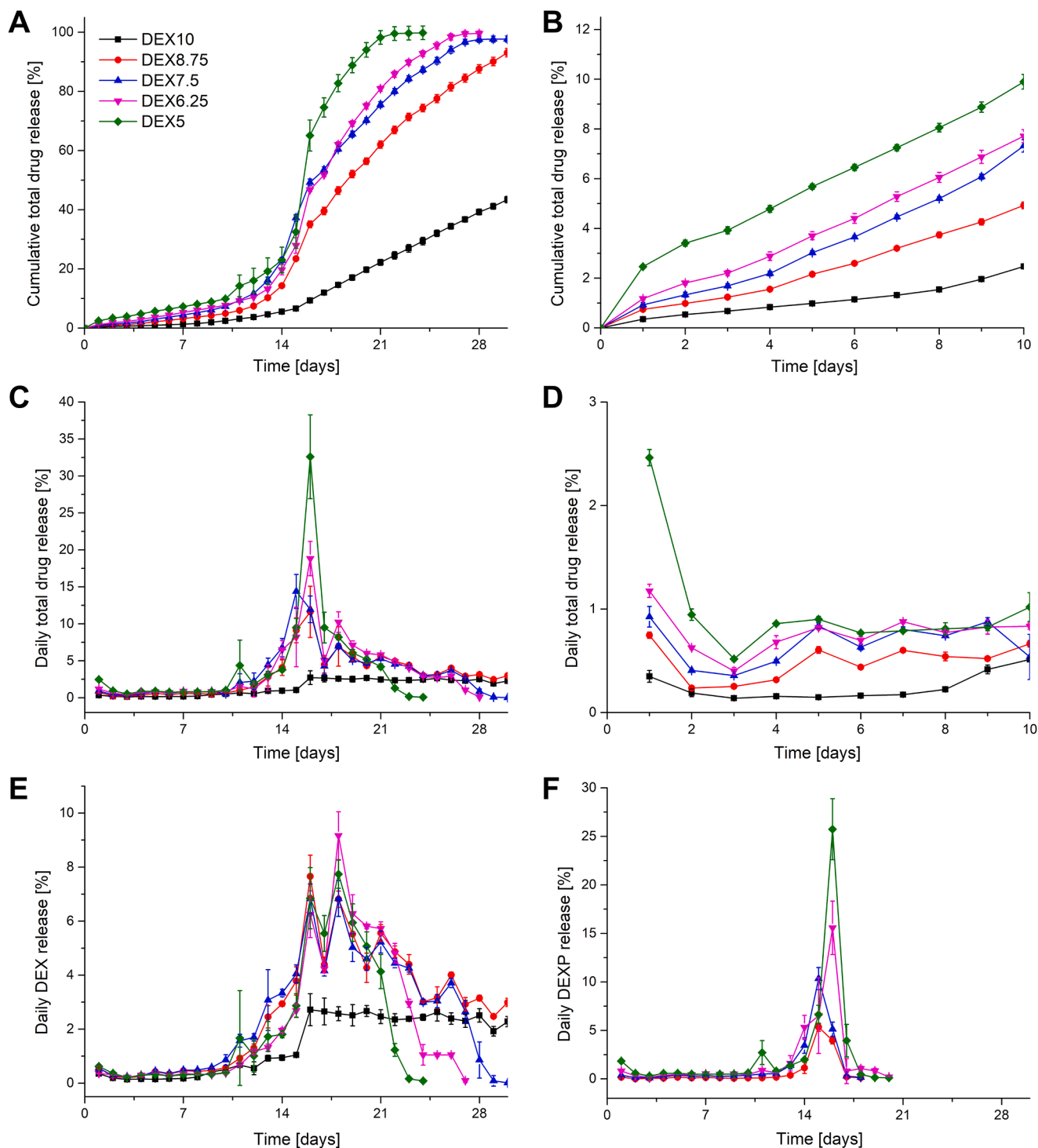


**Fig. 5.** In vitro drug release profiles of implants in phosphate buffer pH 7.4 at 37 °C. Cumulative total drug release (A) and daily total drug release (C) over 28 days, with a closer view of the first 10 days (B, D). Daily release of DEX (E) and DEXP (F) relative to the total drug load. Data are presented as mean  $\pm$  SD,  $n = 3$ .

surface and the increased solubility of DEXP. For all implants, the accelerated drug release phase began around day 16, with significantly higher daily release rates. A higher DEXP content correlated with a higher maximum daily release. For DEX10, the daily release jumped from 1.1 % to 2.7 % during this period, while for DEX5, a massive rise to 32.6 % was measured. Comparing the drug release profiles revealed that even minimal additions of DEXP significantly enhanced DEX release (Fig. 5E). The amount of DEXP added did not seem to influence the overall DEX release rate. As a result, the release of implants containing the lowest absolute amount of DEX (DEX5) was completed after just 24

days. An increase in DEX loading also extended its release duration to 36 days for DEX8.75 implants and up to 84 days for DEXP-free implants (Table 2, Supplementary Figure 1). The daily DEX release displayed a different trend. During the period of maximum drug release, higher DEXP content correlated with a higher daily release (Fig. 5F). Therefore, the presence of DEXP crystals, as identified in the XRD analysis, seems to have no effect on the drug release. However, the DEXP release ended abruptly, with DEX8.75 releasing DEXP for only 17 days, whereas DEX5 released DEXP for 23 days (Table 2). The rapid release of DEXP could also explain the increased release of DEX. The release of DEXP likely

**Table 2**

Cumulative DEXP and DEX content relative to total drug load, along with the corresponding average time required for complete release.

Implant	DEXP			DEX		
	Theoretical [%]	Measured [%]	Duration [days]	Theoretical [%]	Measured [%]	Duration [days]
DEX10	–	–	–	100	98.4 ± 1.5	84
DEX8.75	12.5	12.3 ± 0.4	17	87.5	87.1 ± 1.0	36
DEX7.5	25	24.4 ± 0.7	18	75	74.2 ± 1.8	30
DEX6.25	37.5	37.9 ± 0.6	20	62.5	61.8 ± 1.5	27
DEX5	50	49.4 ± 1.3	23	50	49.7 ± 0.9	24

increased porosity and enhanced water uptake due to its higher hydrophilicity. The increased DEX release rate may be due to van der Waals interactions between DEX and DEXP molecules. These interactions may create a co-transport effect, with DEXP molecules "pulling" DEX molecules out of the matrix.

It is essential to recognize that DEXP is a prodrug, requiring conversion to its active form DEX by enzymes, e.g. phosphatases. However, activation can also occur within the DDS following water uptake and subsequent hydrolysis. Furthermore, enzyme-free conversion within the *in vitro* release medium is possible (Sulaiman et al., 2014; Yi et al., 2015). Daily sampling was crucial to minimize errors from potential conversion in the release medium and to measure the 'true' release of DEXP. Notably, no conversion was observed in any DEXP-containing implants, as the measured cumulative concentration at completed drug release corresponded to the actual loading and determined drug load (Table 2; Fig. 4). This observation proved that DEXP maintained

stability in PEG-PLGA implants throughout the complete release process. For further studies on dose-effect relationships, it must be considered when using dexamethasone phosphate disodium salt that the active part constitutes only 76 % of the total drug amount. For example, in DEX5 implants, only 8.8 % of the 10 % total drug loading exhibits pharmacologically active properties. In summary, the release rate could be increased by the addition of DEXP in the initial days, but at the cost of long-term controlled release.

### 3.3. Degradation characteristics

The drug release data emphasize the need for further investigation to understand the underlying mechanisms during incubation. In theory, incorporating the more hydrophilic DEXP would enhance water penetration, increase swelling, and accelerate drug release. To more deeply characterize matrix degradation, implants were incubated in 12-well

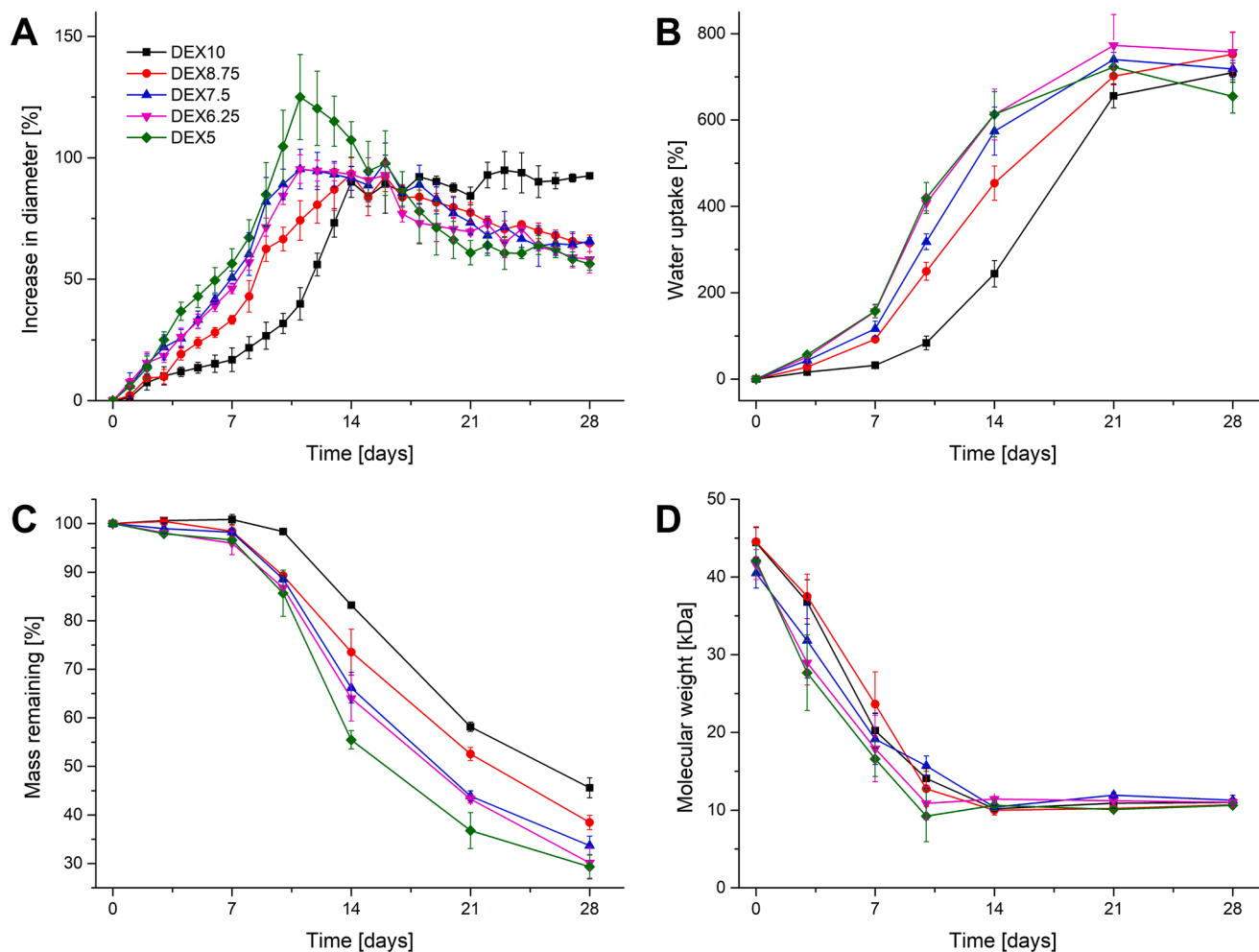


**Fig. 6.** Fate of PEG-PLGA implants upon exposure to PBS 7.4 at 37 °C. Time-dependent changes in diameter (A) and progression of water uptake (B), along with the corresponding erosion (C) and degradation (D). Data are presented as mean ± SD,  $n = 3$ .

cell culture plates and handled carefully to minimize the risk of fragmentation. Fig. 6 shows the fate of PEG-PLGA implants upon exposure to PBS 7.4 at 37 °C. The different implants revealed similar behavior, with a continuous increase in diameter (Fig. 6A). The rate and magnitude of swelling were directly correlated with DEXP concentration. Exemplary, DEX5 exhibited a 125 % increase in diameter within 11 days, while DEX10 reached a 90 % increase after 14 days. Notably, the swelling of DEX10 remained unchanged beyond 28 days. In contrast, implants containing DEXP gradually decreased in diameter over time after reaching their maximum size. The water absorption profile closely mirrored the observed swelling behavior (Fig. 6B). Implants containing DEXP exhibited a more rapid water absorption compared to the DEX10 counterpart. Additionally, the water uptake and swelling patterns in DEXP-containing implants were more linear. Maximum water absorption was achieved by day 21, with no significant differences observed among the implants. Surprisingly, the peak water absorption occurred slightly after the maximum swelling. This temporal offset suggests that water binding to the PEG side chains becomes more prominent once the implants have reached their full expansion. Fig. 6C depicts implant mass loss, with no significant differences observed until day 7. However, a notable increase in mass loss was evident in DEXP-containing implants by day 10. This trend persisted, with the amount of mass loss correlating positively with DEXP content. By day 28, DEX5 retained only 29.3 % of its initial mass, while DEX10 retained 45.6 %. The onset of substantial mass loss coincided with the observed decrease in molecular weight (Fig. 6D). The limited penetration of water into the implants initiated polymer degradation from the beginning upon incubation. After approximately 10 days, the polymer molecular weight decreased to a critical threshold of around 10 kDa, facilitating the dissolution and diffusion of short polymer chains. This process, coupled with the drug release profiles, accounted for the observed mass loss. However, the addition of DEXP had minimal impact on molecular weight reduction, confirming that the observed swelling, water uptake, mass loss, and drug release were predominantly due to the presence of DEXP rather than polymer degradation. Overall, water uptake was limited during the initial days, resulting in low polymer permeability and restricted drug release. Once critical thresholds for water uptake and molecular weight reduction were reached, the drug release rate increased sharply (Fig. 5). This biphasic drug release is typical behavior for PLGA-based implants (Bassand et al., 2022b; Bode et al., 2019; Wachowiak et al., 2023; Zlomke et al., 2019). In general, PEG-PLGA implants showed a more continuously degradation and drug release pattern (Mäder, 2021; Witt et al., 2000). However, the addition of water-soluble DEXP increased the hydrophilicity of the PEG-PLGA implant, facilitating water uptake and thereby accelerating drug release, which led to a transition to a more sigmoidal release profile.

<sup>1</sup>H NMR was utilized to investigate whether polymer degradation occurred preferentially in certain regions and to assess whether the incorporation of DEXP caused detectable variations in degradation behavior. NMR is a powerful tool for quantifying the monomers lactic acid (LA) and glycolic acid (GA) of polymers like PLGA, and in case of PEG-PLGA, also the ethylene glycol (EG) monomers (de Souza et al., 2021; Jeong et al., 2000; Sun et al., 2022). Fig. 7 illustrates a significant change in polymer composition during degradation, demonstrated with DEX10 implants. Specifically, the peak heights of methine (a, 5.2 ppm) and methyl (d, 1.55 ppm) groups of the LA monomers increased relative to the methylene peaks (c, 3.6 ppm) of the EG monomers and to the methylene peaks (b, 4.8 ppm) of the GA monomers. Minor peaks at 1 ppm are attributed to DEX. No signals from DEXP were observed, as DEXP is insoluble in CDCl<sub>3</sub>. New peaks at 1.3 and 4.5 ppm observed after several days of incubation suggest the formation of LA and GA end groups due to polymer cleavage.

The changes in polymer monomers and their ratios as a function of degradation time are plotted in Fig. 8. Although a significantly accelerated mass loss and a smaller effect on molar mass reduction were observed with the addition of DEXP (Fig. 6), no consistent trends were

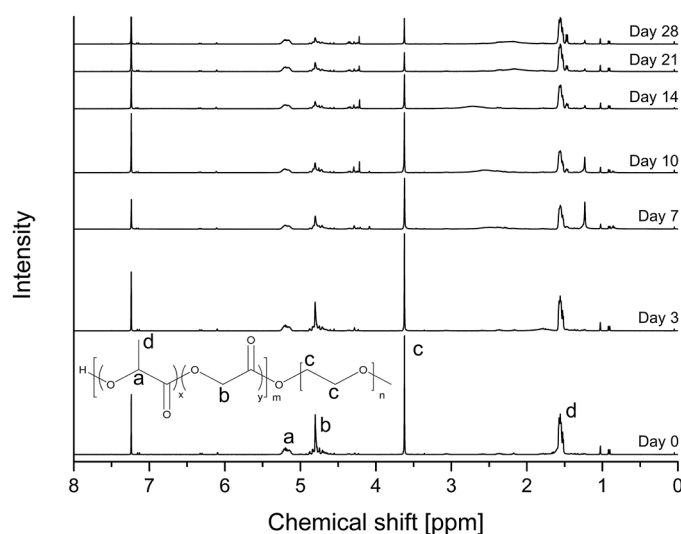
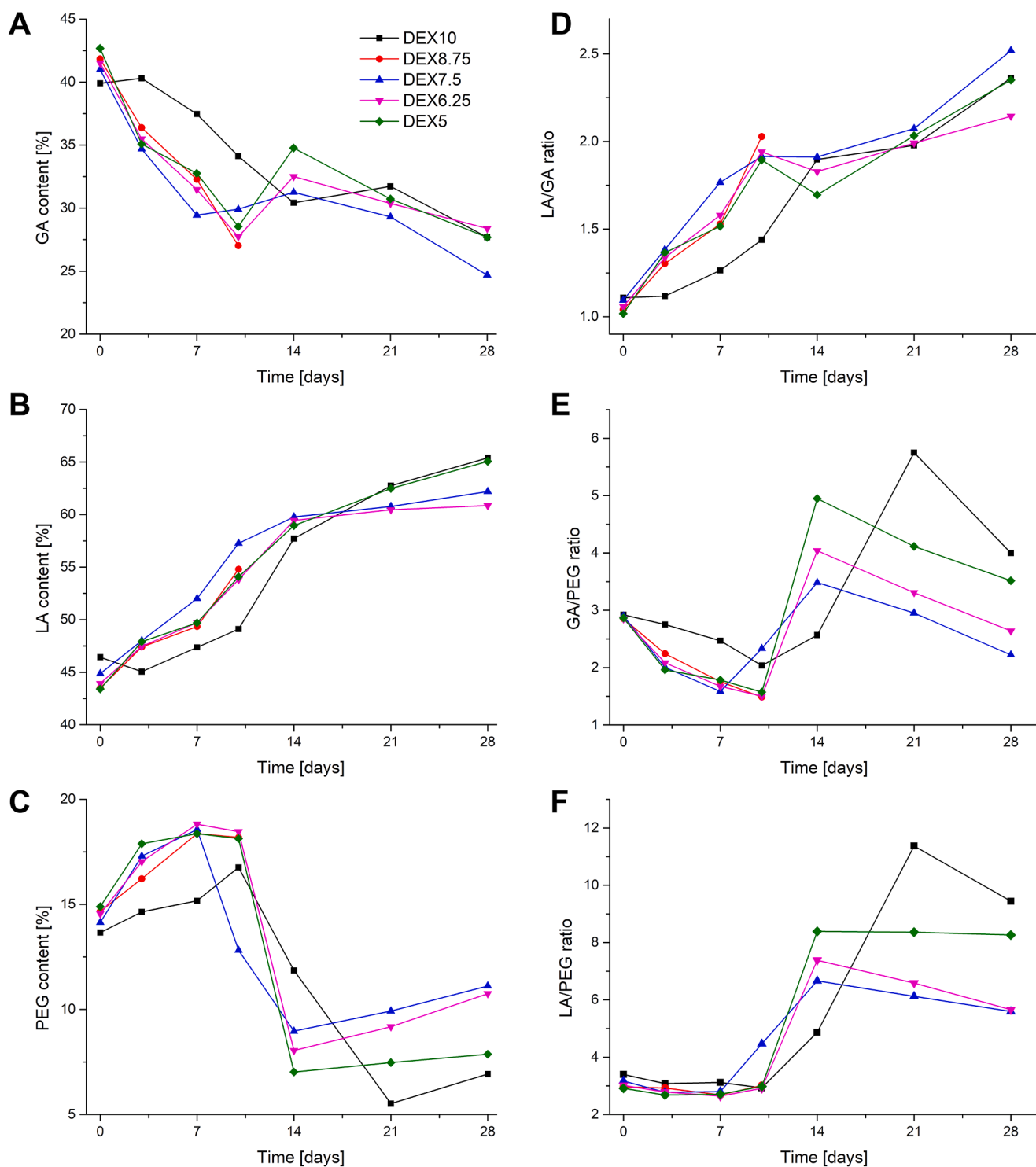


Fig. 7. Changes in <sup>1</sup>H-NMR spectra exemplified by DEX10 implants during degradation over 28 days. Labels correspond to the characteristic proton peaks of PEG-PLGA: CH (a) and CH<sub>3</sub> (d) for lactic acid, CH<sub>2</sub> (b) for glycolic acid, and CH<sub>2</sub> (c) for ethylene glycol.

observed in the changes of polymer units or their ratios in implants containing DEXP. Only the DEXP-free implant variant DEX10 showed a trend in slower GA reduction (Fig. 8A). This can be attributed to the significantly slower water absorption, which delayed the degradation of GA units. However, a continuous reduction in GA was observed for all implant formulations. In contrast, LA monomers were less affected by degradation, resulting in an increase in the percentage of LA monomers in the polymer during the degradation process (Fig. 8B). The increased reactivity of GA monomers has been previously studied, with findings showing that the degradation rate of GA units is 1.3 times higher than that of LA units (Vey et al., 2011). Additionally, the arrangement of the monomers plays a significant role. A greater proportion of the more hydrophilic GA-GA blocks compared to those of the GA-LA and LA-LA blocks is expected to enhance water uptake in PLGA, leading to a relatively faster hydrolysis rate (Sun et al., 2022). The PEG content initially increased slightly due to loss of GA but showed a sharp decrease on day 14 (Fig. 8C). The most significant change was observed in DEX5, with a decrease from 18.1 % to 7.0 %. Once critical thresholds for water uptake and molecular weight were reached (Fig. 6), PEG and low molecular weight PEG-PLGA chains diffused out of the matrix. Since PEG is not biodegradable, it can only be eliminated through diffusion. It should be noted that the implants underwent electron beam irradiation. Recent studies have observed a reduction in the molecular weight of PEG-PLGA following irradiation. (Dorati et al., 2008; Lehner et al., 2023). This reduction can impact the mechanical properties and drug release kinetics. Degradation could be minimized when irradiation is conducted under an argon atmosphere, vacuum, or at reduced temperatures (e.g., liquid nitrogen) (Fintzou et al., 2007). Despite this, no changes in polymer composition were observed after the sterilization process. Before sterilization, the polymer consisted of GA, LA, and PEG in proportions of 41.3 %, 44.4 %, and 14.2 %, respectively (data not shown). However, it has been demonstrated that gamma irradiation induces new <sup>1</sup>H NMR peaks as a result of PEG fragmentation (Dorati et al., 2008). The calculated L/G ratio was consistent with the labeled L/G ratio of the used PEG-PLGA polymer (Fig. 8D). Owing to the accelerated degradation of GA monomers, the L/G ratio steadily increased throughout the incubation period. This observation is in line with previous studies (Saraf et al., 2023; Tang and Singh, 2008). In DEX10 implants, the increase in ratios was considerably more gradual up to day 14 due to the slower degradation of the GA units. The GA/PEG and LA/PEG ratios exhibited a sharp rise at day 14 due to the abrupt decrease in PEG



**Fig. 8.** Time-dependent changes in PEG-PLGA composition during degradation measured by  $^1\text{H-NMR}$ . Calculated molar percentages of glycolic acid (A), lactic acid (B), and polyethylene glycol (C), respectively, with the corresponding monomer ratios (D-F).

content (Fig. 8E, F). However, the transition was less pronounced for GA compared to LA, because of the parallel loss of GA. The role of DEXP in influencing mass loss and water uptake was confirmed by  $^1\text{H-NMR}$  analysis. For DEX8.75, measurements could not be performed after day 14 due to handling challenges with the fragile samples.

#### 4. Conclusion

This study investigated the potential of incorporating hydrophilic

DEXP into PEG-PLGA implants to enhance the initial release of DEX. The addition of DEXP significantly accelerated early drug release, with a maximum fourfold increase observed within the first 10 days. The water-soluble DEXP molecules likely facilitated the diffusion of DEX molecules from the matrix by increasing the hydrophilicity of the system, as demonstrated by enhanced swelling, water uptake, and mass degradation. However, the overall release time was significantly reduced by the addition of DEXP. These results underscore the trade-off between rapid initial release and prolonged, sustained delivery. Further

research is needed to optimize the balance between early release rates and extended drug delivery.

## Funding

This research did not receive any specific grant from funding agencies in the public, commercial, or not-for-profit sectors.

## CRediT authorship contribution statement

**Eric Lehner:** Writing – original draft, Visualization, Methodology, Investigation, Formal analysis, Conceptualization. **Marie-Luise Trutschel:** Methodology, Investigation, Formal analysis. **Matthias Menzel:** Visualization, Investigation, Formal analysis. **Jonas Jacobs:** Investigation, Formal analysis. **Julian Kunert:** Investigation, Formal analysis. **Jonas Scheffler:** Visualization, Investigation, Formal analysis. **Wolfgang H. Binder:** Writing – review & editing, Methodology, Investigation, Formal analysis. **Christian E.H. Schmelzer:** Writing – review & editing, Resources, Conceptualization. **Stefan K. Plontke:** Writing – review & editing, Resources, Conceptualization. **Arne Liebau:** Writing – review & editing, Investigation, Conceptualization. **Karsten Mäder:** Writing – review & editing, Resources, Conceptualization.

## Declaration of competing interest

The authors declare that they have no known competing financial interests or personal relationships that could have appeared to influence the work reported in this paper.

## Acknowledgments

We are thankful to Dr. Wolfgang Knolle from the Leibniz Institute of Surface Engineering (IOM) in Leipzig for sample irradiation. Additionally, we appreciate the assistance provided by Dr. Joana Heinzelmann from the Department of Ophthalmology, Martin Luther University Halle-Wittenberg, in conducting microscopic measurements.

## Supplementary materials

Supplementary material associated with this article can be found, in the online version, at [doi:10.1016/j.ejps.2025.107067](https://doi.org/10.1016/j.ejps.2025.107067).

## Data availability

Data will be made available on request.

## References

- AlAani, H., Alnukkary, Y., 2016. Stability-indicating HPLC method for simultaneous determination of chloramphenicol, dexamethasone sodium phosphate and tetrahydrozoline hydrochloride in ophthalmic solution. *Adv. Pharm. Bull.* 6, 137–141. <https://doi.org/10.15171/apb.2016.020>.
- Anderson, J.M., Shive, M.S., 1997. Biodegradation and biocompatibility of PLA and PLGA microspheres. *Adv. Drug Deliv. Rev.*
- Bassand, C., Freitag, J., Benabed, L., Verin, J., Siepmann, F., Siepmann, J., 2022. PLGA implants for controlled drug release: impact of the diameter. *Eur. J. Pharmac. Biopharmac.* 177, 50–60. <https://doi.org/10.1016/J.EJPB.2022.05.020>.
- Bendicho-Lavilla, C., Seoane-Viaño, I., Santos-Rosales, V., Díaz-Tomé, V., Carracedo-Pérez, M., Luzardo-Álvarez, A.M., García-González, C.A., Otero-Espinar, F.J., 2023. Intravitreal implants manufactured by supercritical foaming for treating retinal diseases. *J. Contr. Rel.* 362, 342–355. <https://doi.org/10.1016/j.jconrel.2023.08.047>.
- Bhagat, R., Zhang, J., Farooq, S., Li, X.-Y., 2014. Comparison of the release profile and pharmacokinetics of intact and fragmented Dexamethasone intravitreal implants in Rabbit eyes. *J. Ocul. Pharmacol. Therap.* 30, 854–858. <https://doi.org/10.1089/jop.2014.0082>.
- Binev, Y., Marques, M.M.B., Aires-de-Sousa, J., 2007. Prediction of <sup>1</sup>H NMR coupling constants with associative neural networks trained for chemical shifts. *J. Chem. Inf. Model.* 47, 2089–2097. <https://doi.org/10.1021/ci700172n>.
- Bode, C., Kranz, H., Fivez, A., Siepmann, F., Siepmann, J., 2019. Often neglected: PLGA/PLA swelling orchestrates drug release: HME implants. *J. Contr. Rel.* 306, 97–107. <https://doi.org/10.1016/j.jconrel.2019.05.039>.
- Bode, C., Kranz, H., Siepmann, F., Siepmann, J., 2018. In-situ forming PLGA implants for intraocular dexamethasone delivery. *Int. J. Pharm.* 548, 337–348. <https://doi.org/10.1016/j.ijpharm.2018.07.013>.
- Costello, M.A., Liu, J., Chen, B., Wang, Y., Qin, B., Xu, X., Li, Q., Lynd, N.A., Zhang, F., 2023. Drug release mechanisms of high-drug-load, melt-extruded dexamethasone intravitreal implants. *Eur. J. Pharmac. Biopharm.* 187, 46–56. <https://doi.org/10.1016/j.ejpb.2023.04.003>.
- de Souza, L.E., Eckenstaler, R., Syrowatka, F., Beck-Broichsitter, M., Benndorf, R.A., Mäder, K., 2021. Has PEG-PLGA advantages for the delivery of hydrophobic drugs? Risperidone as an example. *J. Drug Deliv. Sci. Technol.* 61, 102239. <https://doi.org/10.1016/j.jddst.2020.102239>.
- Dorati, R., Colonna, C., Serra, M., Genta, I., Modena, T., Pavanetto, F., Perugini, P., Conti, B., 2008.  $\gamma$ -irradiation of PEGd,PLA and PEG-PLGA multiblock copolymers: I. effect of irradiation doses. *AAPS. PharmSciTech.* 9, 718–725. <https://doi.org/10.1208/s12249-008-9103-3>.
- Fintzou, A.T., Kontominas, M.G., Badeka, A.V., Stahl, M.R., Riganakos, K.A., 2007. Effect of electron-beam and gamma-irradiation on physicochemical and mechanical properties of polypropylene syringes as a function of irradiation dose: study under vacuum. *Radiat. Phys. Chem.* 76, 1147–1155. <https://doi.org/10.1016/J.RADPHYSHEM.2006.11.009>.
- Fredenberg, S., Wahlgren, M., Reslow, M., Axelsson, A., 2011. The mechanisms of drug release in poly(lactic-co-glycolic acid)-based drug delivery systems - A review. *Int. J. Pharm.* <https://doi.org/10.1016/j.ijpharm.2011.05.049>.
- Gentile, P., Chiono, V., Carmagnola, I., Hatton, P.V., 2014. An overview of poly(lactic-co-glycolic Acid (PLGA)-based biomaterials for bone tissue engineering. *Int. J. Mol. Sci.* <https://doi.org/10.3390/ijms15033640>.
- Janich, C., Friedmann, A., e Silva, J.M.de S., de Oliveira, C.S., de Souza, L.E., Rujescu, D., Hildebrandt, C., Beck-Broichsitter, M., Schmelzer, C.E.H., Mäder, K., 2019. Risperidone-loaded PLGA-lipid particles with improved release kinetics: manufacturing and detailed characterization by electron microscopy and nano-CT. *Pharmaceutics*. 11. <https://doi.org/10.3390/pharmaceutics11120665>.
- Jeong, B., Bae, Y.H., Kim, S.W., 2000. In situ gelation of PEG-PLGA-PEG triblock copolymer aqueous solutions and degradation thereof. *J. Biomed. Mater. Res.* 50, 171–177. [https://doi.org/10.1002/\(SICI\)1097-4636\(200005\)50:2<171::AID-JBMM1>3.0.CO;2-F](https://doi.org/10.1002/(SICI)1097-4636(200005)50:2<171::AID-JBMM1>3.0.CO;2-F).
- Kapoor, D.N., Bhatia, A., Kaur, R., Sharma, R., Kaur, G., Dhawan, S., 2015. PLGA: a unique polymer for drug delivery. *Ther. Deliv.* <https://doi.org/10.4155/tde.14.91>.
- Klose, D., Siepmann, F., Elkharraz, K., Siepmann, J., 2008. PLGA-based drug delivery systems: importance of the type of drug and device geometry. *Int. J. Pharm.* 354, 95–103. <https://doi.org/10.1016/j.ijpharm.2007.10.030>.
- Lehner, E., Gündel, D., Liebau, A., Plontke, S.K., Mäder, K., 2019. Intracochlear PLGA based implants for dexamethasone release: challenges and solutions. *Int. J. Pharm.* X. 1. <https://doi.org/10.1016/j.ijpx.2019.100015>.
- Lehner, E., Honeder, C., Knolle, W., Binder, W., Scheffler, J., Plontke, S.K., Liebau, A., Mäder, K., 2023. Towards the optimization of drug delivery to the cochlear apex: influence of polymer and drug selection in biodegradable intracochlear implants. *Int. J. Pharm.* 643. <https://doi.org/10.1016/j.ijpharm.2023.123268>.
- Lehner, E., Liebau, A., Menzel, M., Schmelzer, C.E.H., Knolle, W., Scheffler, J., Binder, W. H., Plontke, S.K., Mäder, K., 2024. Characterization of PLGA versus PEG-PLGA intracochlear drug delivery implants: degradation kinetics, morphological changes, and pH alterations. *J. Drug Deliv. Sci. Technol.* 99. <https://doi.org/10.1016/j.jddst.2024.105972>.
- Lehner, E., Menzel, M., Gündel, D., Plontke, S.K., Mäder, K., Klehm, J., Kielstein, H., Liebau, A., 2022. Microimaging of a novel intracochlear drug delivery device in combination with cochlear implants in the human inner ear. *Drug Deliv. Transl. Res.* 12, 257–266. <https://doi.org/10.1007/S13346-021-00914-9>.
- MacFhionnghaile, P., Hu, Y., Gniado, K., Curran, S., McArdle, P., Erxleben, A., 2014. Effects of ball-milling and cryomilling on sulfamerazine polymorphs: a quantitative study. *J. Pharm. Sci.* 103, 1766–1778. <https://doi.org/10.1002/jps.23978>.
- Mäder, K., 2021. Characterization methodologies for long-acting and implantable drug delivery systems. *Long-Acting Drug Delivery Systems: Pharmaceutical, Clinical, and Regulatory Aspects*. Elsevier, pp. 319–345. <https://doi.org/10.1016/B978-0-12-821749-8.00001-X>.
- McConville, C., Tawari, P., Wang, W., 2015. Hot melt extruded and injection moulded disulfiram-loaded PLGA millirods for the treatment of glioblastoma multiforme via stereotactic injection. *Int. J. Pharm.* 494, 73–82. <https://doi.org/10.1016/j.ijpharm.2015.07.072>.
- Milacic, V., Schwendeman, S.P., 2014. Lysozyme release and polymer erosion behavior of injectable implants prepared from plga-peg block copolymers and plga/peg blends. *Pharm. Res.* 31, 436–448. <https://doi.org/10.1007/s11095-013-1173-6>.
- Murdande, S.B., Pikal, M.J., Shanker, R.M., Bogner, R.H., 2010. Solubility advantage of amorphous pharmaceuticals: I. a thermodynamic analysis. *J. Pharm. Sci.* 99, 1254–1264. <https://doi.org/10.1002/jps.21903>.
- nmrdb.org. Tools for NMR spectroscopists <https://www.nmrdb.org/> (accessed 15.10.2024).
- Oliveira, P.F.M., Willart, J.F., Siepmann, J., Siepmann, F., Descamps, M., 2018. Using milling to explore physical states: the amorphous and polymorphic forms of dexamethasone. *Cryst. Growth Des.* 18, 1748–1757. <https://doi.org/10.1021/acs.cgd.7b01664>.
- Park, T.G., 1994. Degradation of poly(D,L-lactic acid) microspheres: effect of molecular weight. *J. Contr. Rel.* 30, 161–173. [https://doi.org/10.1016/0168-3659\(94\)90263-1](https://doi.org/10.1016/0168-3659(94)90263-1).

- Patel, B., Gupta, V., Ahsan, F., 2012. PEG-PLGA based large porous particles for pulmonary delivery of a highly soluble drug, low molecular weight heparin. *J. Contr. Rel.* 162, 310–320. <https://doi.org/10.1016/j.jconrel.2012.07.003>.
- Qnouch, A., Solarczyk, V., Verin, J., Tourrel, G., Stahl, P., Danede, F., Willart, J.F., Lemesre, P.E., Vincent, C., Siepmann, J., Siepmann, F., 2021. Dexamethasone-loaded cochlear implants: how to provide a desired “burst release”. *Int. J. Pharm.* X 3, 100088. <https://doi.org/10.1016/J.IJPX.2021.100088>.
- Salt, A.N., Hartsock, J.J., Piu, F., Hou, J., 2018. Dexamethasone and Dexamethasone phosphate entry into perilymph compared for middle ear applications in Guinea pigs. *Audiol. Neurotol.* 23, 245–257. <https://doi.org/10.1159/000493846>.
- Saraf, I., Kushwah, V., Alva, C., Koutsamanis, I., Rattenberger, J., Schroettner, H., Mayrhofer, C., Modhave, D., Braun, M., Werner, B., Zangger, K., Paudel, A., 2023. Influence of PLGA end groups on the release profile of Dexamethasone from ocular implants. *Mol. Pharm.* 20, 1307–1322. <https://doi.org/10.1021/acs.molpharmaceut.2c00945>.
- Šnejdrová, E., Martiška, J., Loskot, J., Paraskevopoulos, G., Kováčik, A., Regdon, G., Budai-Szűcs, M., Palát, K., Konečná, K., 2021. PLGA based film forming systems for superficial fungal infections treatment. *Eur. J. Pharm. Sci.* 163. <https://doi.org/10.1016/j.ejps.2021.105855>.
- Steele, T.W.J., Huang, C.L., Widjaja, E., Boey, F.Y.C., Loo, J.S.C., Venkatraman, S.S., 2011. The effect of polyethylene glycol structure on paclitaxel drug release and mechanical properties of PLGA thin films. *Acta Biomater.* 7, 1973–1983. <https://doi.org/10.1016/j.actbio.2011.02.002>.
- Sulaiman, S., Khamis, M., Nir, S., Lelario, F., Scrano, L., Bufo, S.A., Karaman, R., 2014. Stability and removal of dexamethasone sodium phosphate from wastewater using modified clays. *Environ. Technol.* 35, 1945–1955. <https://doi.org/10.1080/09593330.2014.888097>.
- Sun, J., Walker, J., Beck-Broichsitter, M., Schwendeman, S.P., 2022. Characterization of commercial PLGAs by NMR spectroscopy. *Drug Deliv. Transl. Res.* 12, 720–729. <https://doi.org/10.1007/s13346-021-01023-3>.
- Tang, Y., Singh, J., 2008. Controlled delivery of aspirin: effect of aspirin on polymer degradation and in vitro release from PLGA based phase sensitive systems. *Int. J. Pharm.* 357, 119–125. <https://doi.org/10.1016/j.ijpharm.2008.01.053>.
- Vey, E., Rodger, C., Booth, J., Claybourn, M., Miller, A.F., Saiani, A., 2011. Degradation kinetics of poly(lactide-co-glycolic) acid block copolymer cast films in phosphate buffer solution as revealed by infrared and raman spectroscopies. *Polym. Degrad. Stab.* 96, 1882–1889. <https://doi.org/10.1016/j.polymdegradstab.2011.07.011>.
- Wachowiak, S., Danede, F., Willart, J.F., Siepmann, F., Siepmann, J., Hamoudi, M., 2023. PLGA implants for controlled dexamethasone delivery: impact of the polymer chemistry. *J. Drug Deliv. Sci. Technol.* 86. <https://doi.org/10.1016/j.jddst.2023.104648>.
- Wang, K., 2012. Die swell of complex polymeric systems. *Viscoelasticity - From Theory to Biological Applications*. IntechOpen. <https://doi.org/10.5772/50137>.
- Webber, W.L., Lago, F., Thanos, C., Mathiowitz, E., 1998. Characterization of soluble salt-loaded, degradable PLGA films and their release of tetracycline. *J. Biomed. Mater. Res.* 41, 18–29. [https://doi.org/10.1002/\(SICI\)1097-4636\(199807\)41:1<18::AID-JBM3>3.0.CO;2-T](https://doi.org/10.1002/(SICI)1097-4636(199807)41:1<18::AID-JBM3>3.0.CO;2-T).
- Wischke, C., Schwendeman, S.P., 2008. Principles of encapsulating hydrophobic drugs in PLA/PLGA microparticles. *Int. J. Pharm.* <https://doi.org/10.1016/j.ijpharm.2008.04.042>.
- Witt, C., Mäder, K., Kissel, T., 2000. The degradation, swelling and erosion properties of biodegradable implants prepared by extrusion or compression moulding of poly(lactide-co-glycolide) and ABA triblock copolymers. *Biomaterials* 21, 931–938. [https://doi.org/10.1016/S0142-9612\(99\)00262-8](https://doi.org/10.1016/S0142-9612(99)00262-8).
- Yi, W., Zhibang, Y., Lili, Z., Zhongquan, S., Lianju, M., Ziwei, T., Renju, J., 2015. Isolation and identification of dexamethasone sodium phosphate degrading *Pseudomonas alcaligenes*. *J. Basic Microbiol.* 55, 262–268. <https://doi.org/10.1002/jobm.201300912>.
- Zhang, C., Bodmeier, R., 2023. Direct drug milling in organic PLGA solution facilitates the encapsulation of nanosized drug into PLGA microparticles. *Eur. J. Pharm. Biopharm.* 191, 1–11. <https://doi.org/10.1016/j.ejpb.2023.08.006>.
- Zhang, Y., Zale, S., Sawyer, L., Bernstein, H., 1997. Effects of metal salts on poly(DL-lactide-co-glycolide) polymer hydrolysis. *J. Biomed. Mater. Res.* 34, 531–538. [https://doi.org/10.1002/\(SICI\)1097-4636\(19970315\)34:4<531::AID-JBM13>3.0.CO;2-F](https://doi.org/10.1002/(SICI)1097-4636(19970315)34:4<531::AID-JBM13>3.0.CO;2-F).
- Zlomke, C., Barth, M., Mäder, K., 2019. Polymer degradation induced drug precipitation in PLGA implants – why less is sometimes more. *Eur. J. Pharm. Biopharm.* 139, 142–152. <https://doi.org/10.1016/J.EJPB.2019.03.016>.